Vietnam Journal of Science and Technology
DOI: https://doi.org/10.15625/2525-2518/22611

Controlled release and drug delivery potential of carrageenan/poly(lactic acid) composites for lovastatin

Vu Quoc Manh[1], Tran Thi Kieu Giang[2], Vu Thi Thuong[2], Doan Thi Yen[2], Bui Thanh Nga[2], Huynh Xuan Mai[2], Pham Nguyen Thao Nguyen[2], Nguyen Thi Hong Nhung[1], Nguyen Ngoc Linh[1], Nguyen Thi Bich Viet[2], Vu Thi Huong[2], Nguyen Dang Dat[2], Vu Quoc Trung[2,*]

[1]*Faculty of Pharmacy, Thanh Do University, Kim Chung, Hoai Duc Ward, Ha Noi, Viet Nam*
[2]*Faculty of Chemistry, Hanoi National University of Education, 136 Xuan Thuy Road, Cau Giay Ward, Ha Noi, Viet Nam*

[*]Email: *trungvq@hnue.edu.vn*

Received: 25 March 2025; Accepted for publication: 1 July 2025

Abstract. This study investigates the efficacy of poly(lactic acid)/carrageenan (PLA/Carr) composites in the encapsulation and controlled release of lovastatin (Lov). PLA/Carr/Lov composites were synthesized via a solution method with varying PLA/Carr ratios. The structural, morphological, thermal, and drug release properties of the composites were analyzed using Fourier-transform infrared spectroscopy (FTIR), scanning electron microscopy (SEM), differential scanning calorimetry (DSC), and ultraviolet-visible (UV-Vis) absorption spectroscopy. The results indicate that Lov was uniformly dispersed within the polymer matrix as nanoparticles ranging from 20 to 220 nm in size. Drug release studies in pH 2.0 and pH 7.4 environments revealed a biphasic release profile, consisting of an initial burst release followed by a sustained release phase. The PLA/Carr significantly influenced drug loading efficiency and release kinetics, with the optimal controlled release observed at a PLA/Carr ratio of 2:8. These findings highlight the potential of Carr/PLA composites as promising carriers for controlled drug delivery applications.

Keywords: carrageenan, poly(lactic acid), lovastatin, drug delivery system, controlled drug release.

Classification numbers: 1.2.4, 2.7.1, 2.9.3.

1. INTRODUCTION

Poly(lactic acid) (PLA) is a biodegradable, biocompatible, non-toxic, and environmentally friendly polymer, making it highly attractive for biomedical and pharmaceutical applications. PLA and its derivatives are widely utilized in medical implants, tissue engineering, orthopedic devices, and drug delivery systems due to their excellent mechanical properties, controlled degradability, and ease of processing [1, 2]. Unlike petroleum-derived polymers, PLA is synthesized from renewable resources such as wheat, corn, and rice, requiring 25–55 % less energy for production, thereby contributing to sustainability efforts [3]. Furthermore, the degradation products of PLA, primarily lactic acid, are non-toxic to both humans and the

environment, reinforcing its suitability for biomedical applications [4]. One of the PLA's key advantages in drug delivery applications is its ability to undergo controlled degradation, enabling sustained and targeted drug release. PLA degrades via hydrolysis into lactic acid, which can be metabolized by the human body without causing toxicity. This property is particularly beneficial in drug delivery systems, where the controlled metabolism of the polymer carrier ensures a consistent therapeutic drug concentration while minimizing side effects [5, 6]. Various approaches have been explored to fabricate PLA-based drug carriers, including the emulsion-solvent evaporation method. For instance, PLA microspheres have been used to encapsulate gentamicin [7], lovastatin (Lov) [8], and mildronate [9], enhancing drug stability, bioavailability and providing sustained or extended release profiles. Additionally, PLA has been chemically modified to conjugate drugs to its distal hydroxyl (–OH) groups, yielding pharmacologically active polymer systems with improved solubility, stability, and combination therapy potential [10]. PLA has also been successfully employed for carrying local anesthetics, such as bupivacaine, demonstrating prolonged drug release compared to poly(lactic-co-glycolic acid) (PLGA) formulations [11].

Carrageenan (Carr) is a naturally occurring polysaccharide derived from various species of red algae, including *Agardhiella, Chondrus crispus, Eucheuma, Furcellaria, Gigartina, Hypnea, Iridaea, Sarconema,* and *Solieria* [12]. These algae contain substantial amounts of Carr in their cell walls, accounting for 30-75 % of their dry weight [13]. Carr has attracted significant attention in biomedical and pharmaceutical research due to its biocompatibility, high molecular weight, viscosity, and gel-forming ability [14]. Beyond its extensive use in the food industry, Carr has become a key biomaterial in drug delivery, where it has been used to improve drug formulations and regulate release kinetics [15–20]. Additionally, Carr exhibits a range of biological activities, including antioxidant [21], antiviral [22–24], antibacterial [25, 26], antihyperlipidemic [27–29], anticoagulant [30, 31], antitumor, and immunomodulatory properties [32–34], further expanding its potential in therapeutic applications. High molecular weight carrageenan (undegraded carrageenan) is not broken down by human digestive enzymes. It is not absorbed into the bloodstream but passes through the digestive tract largely intact and is excreted in the feces [35]. A small portion may undergo fermentation by colonic microbiota, but this is considered negligible [36].

Lovastatin (Lov) is a naturally occurring statin primarily found in oyster mushrooms (Pleurotus ostreatus) [37] and red yeast rice (rice fermented by Monascus) [38]. It is widely recognized as one of the most effective cholesterol-lowering agents, functioning by inhibiting the enzyme 3-hydroxy-3-methylglutaryl-CoA (HMG-CoA) reductase, a key enzyme in cholesterol biosynthesis [39]. Lov selectively reduces low-density lipoprotein (LDL) levels while maintaining high-density lipoprotein (HDL) concentrations, contributing to its cardioprotective effects. Clinical studies have demonstrated that Lov significantly reduces mortality associated with coronary heart disease [8]. However, the therapeutic effectiveness of Lov is limited by its poor water solubility, resulting in low bioavailability (~5 %) and rapid metabolism, with peak plasma concentrations occurring within 4 hours and a half-life of approximately 3 hours [40]. When adding Lov into polymeric matrices, such as alginate/chitosan [41], chitosan/carrageenan polyaniline [42], chitosan/carrageenan [43], PLA [44], collagen [45], its dispersion, stability, and controlled release properties could be enhanced.

To exploit the synergistic properties of both PLA and Carr, the present study focuses on developing and characterizing a novel Carr/PLA composite system for Lov loading and release. This study also aims to evaluate the potential of the Carr/PLA system in improving Lov solubility, release kinetics, and therapeutic efficiency. The findings from this research could contribute to

the development of advanced polymer-based drug delivery platforms for Lov and other hydrophobic drugs.

2. MATERIALS AND METHODS

2.1. Materials

Carrageenan (Carr) (in powder; containing ≤ 2 % sodium, ≤ 3.5 % calcium, ≤ 11 % potassium; pH (1.5 % in H_2O) of 7.5–10.5; predominantly κ-Carr and a small amount of λ-Carr) and poly(lactic acid) (Mw: 67000 g/mol, melting point: 264–269 °C) were provided by Sigma-Aldrich (USA). Dry powder lovastatin (≥ 98 %) was purchased from Rhawn (China). Other chemicals such as C_2H_5OH, HCl, KCl, CH_3COOH, KH_2PO_4, Na_2HPO_4, CH_3COONa, were of analytical grades.

2.2. Preparation of lovastatin-loaded PLA/Carr/Lov (PCL) composites

The samples were prepared in the laboratory at a room temperature of 25 °C and a relative humidity of 50 %.

PLA/Carr/Lov (PCL) biocomposite samples were prepared using the solution method by varying the PLA/Carr ratio to determine the optimal composition (see Table 1). The synthesis followed these steps: PLA was dissolved in dichloromethane (DCM) at a concentration of 1 g per 100 mL (PLA/DCM, w/v) to produce solution A. Separately, Carr was dissolved in hot water at 80 °C with a concentration of 1 g per 200 mL (Carr/water, w/v) under continuous stirring for 30 minutes. The solution was then cooled to 30 °C to obtain solution B. Lov was dissolved ethanol using a magnetic stirrer to form solution C.

Solution B was gradually added to solution A at a controlled rate of 20 drops per minute, followed by homogenization at 20,000 rpm to obtain emulsion D [46]. Emulsion D was then stirred on a magnetic stirrer at 400 rpm for 1.5 hours. Carr functions as an effective emulsifier by increasing the viscosity of the aqueous phase through its gel-forming ability and ionic interactions. The presence of Na^+ and K^+ ions in carrageenan facilitates the formation of an ion–water network, which enhances water retention and uniformly disperses carrageenan in solution. This network not only supports gel structure formation but also inhibits droplet coalescence and phase separation of the oil phase (PLA in DCM) by stabilizing the interface and increasing continuous phase viscosity. As a result, carrageenan effectively retards creaming and maintains emulsion stability [12, 20, 42]. Subsequently, solution C was added dropwise to emulsion D at the same rate (20 drops/minute) while homogenizing at 20,000 rpm. The resulting mixture underwent additional stirring at 400 rpm for 1 hour. Finally, the prepared mixture was poured into a Petri dish and allowed to evaporate naturally over 48 hours, forming the PLA/Carr/Lov composite. After preparation, the samples were stored in zip-lock (PE) bags and kept in a refrigerator at a temperature of 4–8 °C, allowing gradual solvent evaporation.

Table 1. Composition of PLA/Carr/Lov composite samples.

No.	Composite sample	PLA (g)	Carr (g)	Lov (g)
1	PCL821	0.4	0.1	0.05
2	PCL641	0.3	0.2	0.05
3	PCL551	0.25	0.25	0.05
4	PCL461	0.2	0.3	0.05
5	PCL281	0.1	0.4	0.05

2.3. Characterization of PLA/Carr/Lov (PCL) biocomposites

The Fourier Transform Infrared (FT-IR) spectra of the biocomposite samples were obtained using a Thermo Nicolet Nexus 670 FT-IR spectrometer by scanning within the range from 400 cm^{-1} to 4000 cm^{-1} with a resolution of 8 cm^{-1}, and a scan number of 32.

The surface morphology of the samples was examined using a Hitachi S-4800 field emission scanning electron microscope (FE-SEM) under nitrogen atmosphere. To prevent surface charging, the samples were coated with a thin platinum layer before imaging. Particle size was determined using ImageJ software version 1.48v.

Thermal properties were analyzed using differential scanning calorimetry (DSC) with a Shimadzu DSC60 instrument. Measurements were performed under a nitrogen atmosphere from 30 °C to 300 °C at a heating rate of 10 °C/min.

The amount of Lov released from the composite samples was quantified using a YOKE UV1900 UV- Vis Double Beam Spectrophotometer.

2.4. Determination of Lov release from the PLA/Carr/Lov (PCL) biocomposites

The drug release behavior of crystalline Lov from the biocomposite samples was evaluated in simulated gastric fluid (pH 2.0) and simulated intestinal fluid (pH 7.4) at 37.0 ± 0.1 °C. Pre-weighed samples were placed in 200 mL of either pH 2.0 or pH 7.4 buffer solution, and the mixture was stirred continuously at 200 rpm using a 6-position dissolution tester. At 1-hour intervals, 5 mL of the solution was withdrawn and immediately replaced with an equal volume of fresh buffer to maintain a constant volume. The sample was continuously tested for 30 hours [47], as the Lovastatin-loaded carrier system exhibits sustained release properties to maintain the minimum plasma concentration [8].

The withdrawn samples were analyzed using a UV–Vis spectrophotometer to record the absorbance (A) of the solution at a λ_{max} of 238.8 nm in pH 2.0 buffer and a λ_{max} of 239.6 nm in pH 7.4 buffer. Each sample was measured three times, and the average value was reported. Each experiment was performed in triplicate. The released Lov concentration (C_{Lov}) in both pH 2.0 and pH 7.4 solutions was determined using the following calibration curve equations:

pH 2.0 solution: $A_{238.8nm} = 1325.7 \times C_{Lov} + 0.0599$ ($R^2 = 0.9916$). Linear range: 1.05–4.75 mg/100 mL; LOD: 7.2×10^{-5} mg/100 mL; LOQ = 2.18×10^{-4} mg/100 mL.

pH 7.4 solution: $A_{239.6nm} = 21956 \times C_{Lov} + 0.0412$ ($R^2 = 0.9951$). Linear range: 1.461–6.757 mg/100 mL; LOD: 8.3×10^{-7} mg/100 mL; LOQ = 3×10^{-6} mg/100 mL.

The percentage of Lov released (H %) from the biocomposite samples in these solutions at a given time was calculated using the equation:

$$H\ (\%) = \frac{m_t}{m_o} \text{ x } 100\ \%$$

where H (%) is the percentage of Lov released at a specific time, m_t is the mass of Lov released at a specific time, and m_o is the initial mass of Lov in the composite sample.

3. RESULTS AND DISCUSSION

3.1. FT-IR spectra of biocomposite materials

The FT-IR spectra of carrageenan (Carr), polylactic acid (PLA) and lovastatin (Lov) are presented in Figure 1. The FT-IR spectrum of Lov exhibits a characteristic absorption band at 3537 cm^{-1}, corresponding to the stretching vibration of the hydroxy (–OH) group. Additionally, absorption bands at 2964 cm^{-1}, 2928 cm^{-1}, and 2865 cm^{-1} are attributed to the stretching vibrations of the C_{sp3}–H. The carbonyl (C=O) stretching vibrations are observed at 1722 cm^{-1} and 1696 cm^{-1}, whereas the C–O bond exhibits a stretching vibration at 1068 cm^{-1} [48].

The FT-IR spectrum of PLA displays prominent absorption bands attributed to the C=O stretching vibration at 1747 cm^{-1}, alongside C_{sp3}–H vibrations at 2994 cm^{-1}, 2950 cm^{-1}, 2913 cm^{-1}, and 2845 cm^{-1}. The C–O stretching vibration is observed at 1081 cm^{-1} [49].

For Carr, the FT-IR spectrum shows a broad absorption band at 3383 cm^{-1}, corresponding to the stretching vibration of the –OH group. A distinct peak at 1634 cm^{-1} is characteristic of the C=O stretching vibration, while the C–O band appears at 1036 cm^{-1}. Additionally, the S=O functional group shows a characteristic vibrational peak at 843 cm^{-1} [20].

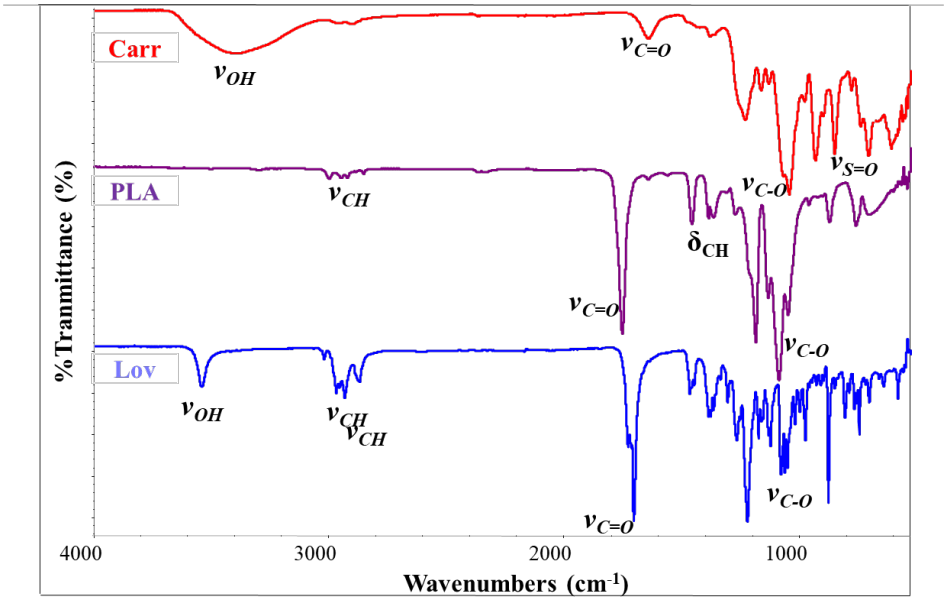

Figure 1. FT-IR spectra of Carr, PLA, and Lov.

The FT-IR spectra of PCL composites are shown in Figure 2, revealing the characteristic absorption bands corresponding to the functional groups of PLA, Carr, and Lov. These characteristic peaks appear in all PCL composites, though slight shifts in wavenumbers are noted compared to the original spectra of PLA, Carr, and Lov.

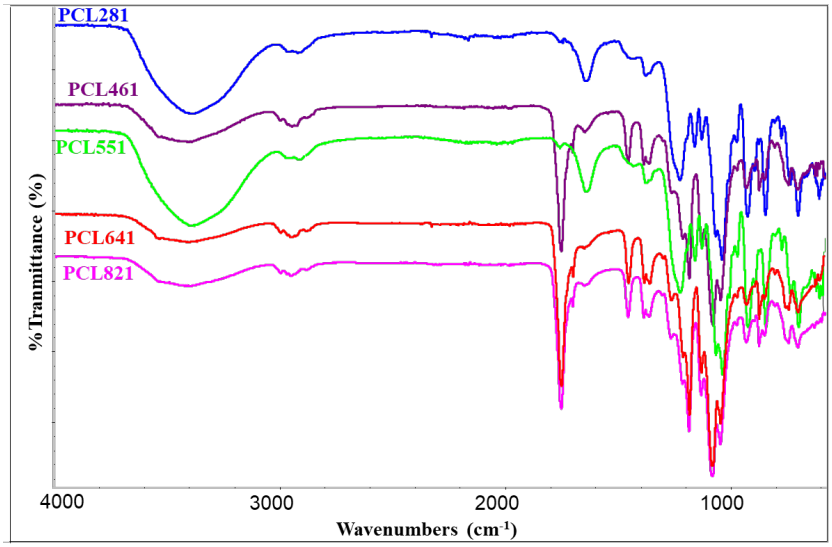

Figure 2. FTIR spectra of PCL composite samples with different PLA/Carr ratios.

For instance, in the PCL281 composite, the absorption band corresponding to the C=O stretching vibration appears at 1639 cm^{-1}, representing a shift of 109 cm^{-1} relative to PLA (1748 cm^{-1}) and 83 cm^{-1} relative to Lov (1722 cm^{-1}). Additionally, the peak associated with the –OH group at 3537 cm^{-1} in the PCL281 composite shifts by 5 cm^{-1} compared to Carr and by 149 cm^{-1} compared to Lov. These spectral shifts suggest strong intermolecular interactions among PLA, Carr, and Lov, primarily through dipole interactions and hydrogen bonding between the C=O group in Lov and the –OH group in Carr [43].

Moreover, variations in the Carr/PLA ratio appear to influence the intensity of absorption bands rather than their position. This indicates that within the PCL composites, Lov interacts physically with other components without altering their chemical structures. As a result, the intrinsic properties of the components, particularly the pharmacological activity of Lov remains unchanged in the composite material.

Table 2 summarizes the characteristic wavenumbers observed in Lov, Carr, PLA, and PCL composites.

Table 2. Characteristic vibrations (cm^{-1}) of Carr, PLA, Lov, and PCL composites.

	Carr	PLA	Lov	PCL281	PCL461	PCL551	PCL641	PCL821
ν_{OH}	3383			3537	3388	3388	3383	3401
$\nu_{CH\ no}$	-	2995 2950 2913 2845	2964 2928 2865	2917	2943	2904	2945	2946
$\nu_{C=O}$	1634	1748	1722 1697	1639	1749	1639	1749	1749
δ_{CH}	1373	1359 1383	1384	1373	1381	1375	1359	1381
ν_{C-O}	1036	1082 1043	1069	1036	1076 1042	1065 1035	1080 1042	1078 1042
$\nu_{S=O}$	843	-	-	842	870	842	870	870

3.2. Morphology of the PLA/Carr/Lov (PCL) biocomposites

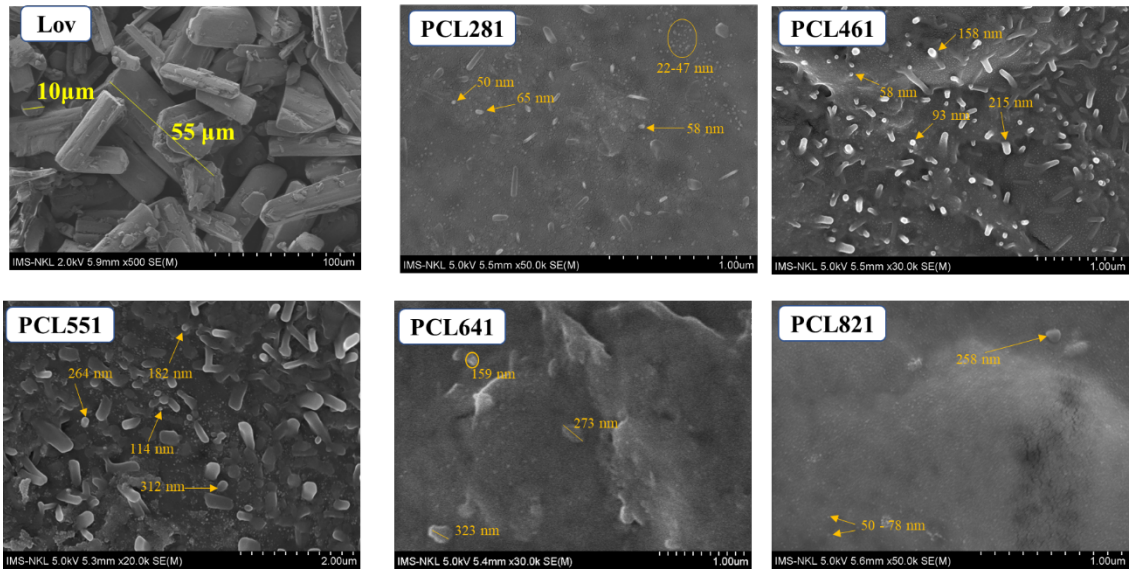

Figure 3. FE-SEM images of Lov and PCL composite samples.

The surface morphology of Lov and PCL samples was examined using SEM images, as shown in Figure 3. SEM images of Lov reveal that it exists in the form of rod-shaped crystals with a relatively large and non-uniform size distribution, ranging from 10 to 55 µm.

In contrast, within the PCL samples, Lov particles dissolve in ethanol during dispersion in the polymer matrix, leading to their transformation into spherical shapes. The dispersion efficiency of Lov within the polymer matrix is influenced by the PLA/Carr ratio, with particle size varying from 22 to 323 nm.

Specifically, SEM analysis of the PCL281 composite indicates that Lov particles exhibit a well-defined spherical morphology, with sizes ranging from 22 to 65 nm, and well dispersed within the polymer matrix. Furthermore, FE-SEM imaging of the PCL281 composite reveals an even dispersion of Lov within the polymer matrix with minimal particle agglomeration, where particle sizes are reduced to the range of 22 - 47 nm. In contrast, for PCL461 and PCL551 samples with a PLA:Carr ratio of approximately 1:1, heterogeneous aggregation may occur, leading to reduced diffusion and release of Lov [20].

This improved dispersion is attributed to strong dipole interactions between the sulfate groups in Carr and the hydrogen bonding between the –C=O group in Lov and the –OH group of Carr [50]. Additionally, PLA forms hydrogen bonds with both Carr and Lov, further facilitating Lov's uniform distribution within the polymer matrix. Moreover, the hydrogen bonding interactions between Lov and the matrix enable Lov particles to integrate into the spatial structure of the composite, enhancing their dispersion within the matrix system.

3.3. Thermal properties of composite materials

The DSC diagrams of Lov and PCL composites with varying Carr/PLA ratios are shown in Figure 4. The DSC thermogram of Lov exhibits a distinct melting endothermic peak at 174.6 °C,

corresponding to its melting point. The melting process initiates at 172 °C and concludes at 177 °C, aligning with previously reported findings [46, 51].

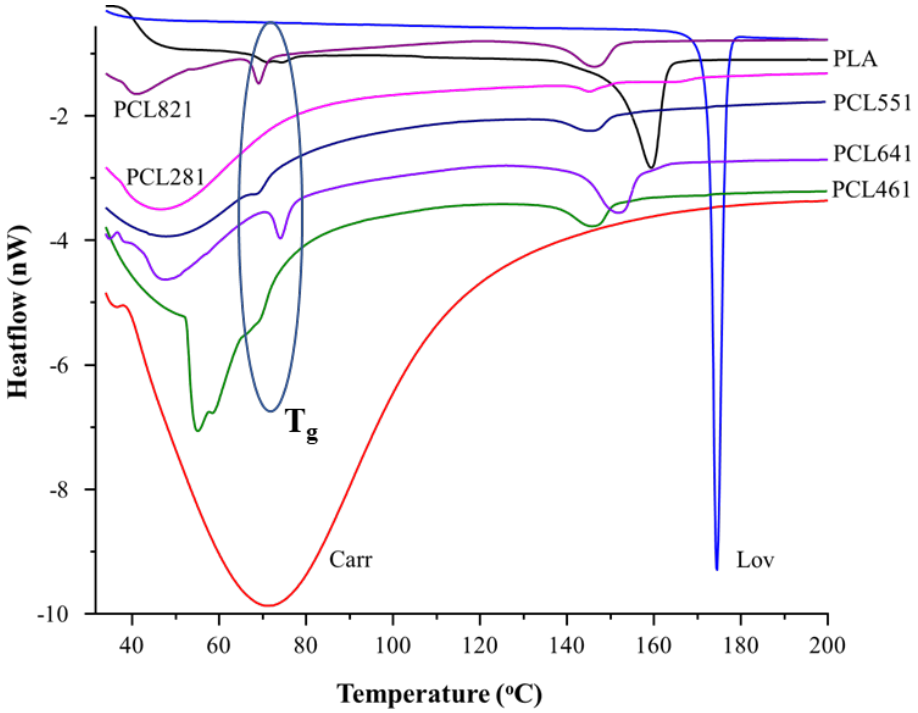

Figure 4. DSC thermograms of Lov and PCL composite samples.

For neat PLA, DSC analysis revealed two distinct thermal transitions at 74.79 °C and 153.72 °C, corresponding to the polymer's glass transition (T_g) and melting temperature (T_m), respectively [52]. In contrast, the DSC thermogram of pure Carr displayed a single prominent endothermic peak at approximately 72.78 °C, associated with its melting point [53]. These results establish the baseline thermal behavior of the individual components. In the DSC profiles of the PLA/Carr composite samples, two main thermal events were observed. The first was a dominant endothermic peak around 72–73 °C, arising from the melting of the Carr component, and the second was a much smaller thermal transition associated with the T_g of PLA. At higher Carr loadings, the melting peak became increasingly pronounced, partially masking the PLA glass transition in the DSC trace. This thermal masking effect is particularly evident in the sample with the highest Carr content (PLC281), where the large Carr melting endotherm significantly diminishes the observable PLA T_g signal.

A notable reduction in Lov's melting point was observed upon incorporation into the Carr/PLA matrix, as evidenced by the shift in the second endothermic peak of the PCL composites. This decrease in melting temperature can be attributed to the transition of Lov from a crystalline to an amorphous state when dispersed within the polymer system, leading to a lower melting temperature compared to its pure crystalline form [42]. These findings are in strong agreement with the SEM results discussed earlier, which indicated uniform dispersion of Lov within the polymer matrix.

DSC analysis revealed that the melting point of Lovastatin (Lov) in the PCL281 sample decreased to 145.26 °C, compared to 174.6 °C in its crystalline form, indicating enhanced

solubility under physiological conditions (pH 7.4). This improved dissolution is attributed to the weakened interactions between Lov and the polymer matrix. Additionally, the swelling behavior of the polymer network - facilitated by the water-retaining and emulsifying properties of carrageenan - further promotes the diffusion of Lov into the surrounding medium [20, 42, 43]. Furthermore, as shown in Table 3, the PCL281 sample exhibits the lowest second endothermic peak temperature (145.26 °C), reinforcing the SEM observations that this sample has the smallest and most uniformly distributed Lov particle within the polymer matrix.

Table 3. DSC results of Lov and PCL composite samples.

Sample	1st peak (°C)	2nd peak (°C)
Lov	-	174.6
PCL281	47.46	145.26
PCL461	54.83	146.6
PCL551	48.52	146.24
PCL641	41.47	146.98
PCL821	40.90	146.66

3.4. Lovastatin release from PCL composite materials

The release profile of Lov from PCL composites with varying Carr/PLA ratios (PCL281, PCL461, PCL551, PCL641, PCL821) in a pH 2.0 buffer solution is presented in Figure 5 (left). As observed, pure Lov exhibits poor solubility and low release efficiency in pH 2.0 buffer, consistent with its inherent solubility and previous studies. However, when Lov is incorporated into the matrix polymer to form PCL composites, its solubility is significantly enhanced.

The improvement in solubility can be attributed to the formation of hydrogen bonds between Lov and the base polymers (PLA and Carr), which facilitate the uniform dispersion of Lov within the polymer system and contribute to a reduction in particle size. Additionally, PLA and Carr interact via hydrogen bonding between the -OH groups of Carr and the C=O groups of PLA, further stabilizing the system.

The drug release profile of Lov exhibits a biphasic pattern: an initial rapid release within the first 10 hours, followed by a slower, controlled release phase. This sustained release behavior helps maintain Lov concentration over an extended period, supporting long-term, therapeutic applications. The enhanced dispersion of Lov in the PLA/Carr matrix, along with its transition to an amorphous form, further improves its solubility in the acidic pH 2.0 environment.

Furthermore, the degradation and gradual disintegration of the polymer matrix facilitate the controlled release of Lov, resulting in a higher cumulative drug release from the PCL composite compared to pure Lov. Notably, the PCL281 composite exhibits the lowest release rate in pH 2.0 buffer, suggesting its potential for protecting Lov in the acidic gastric environment, where drug absorption is minimal.

Similar to the observations in pH 2.0 buffer, the release of Lov in pH 7.4 buffer solution, as shown in Figure 5-right, was significantly higher from the PCL composite samples compared to pure Lov. After 30 hours of testing [46], the cumulative release of Lov from PCL281, PCL461, PCL551, PCL641, and PCL821 in pH 7.4 buffer solution were markedly greater than that in pH 2.0 buffer.

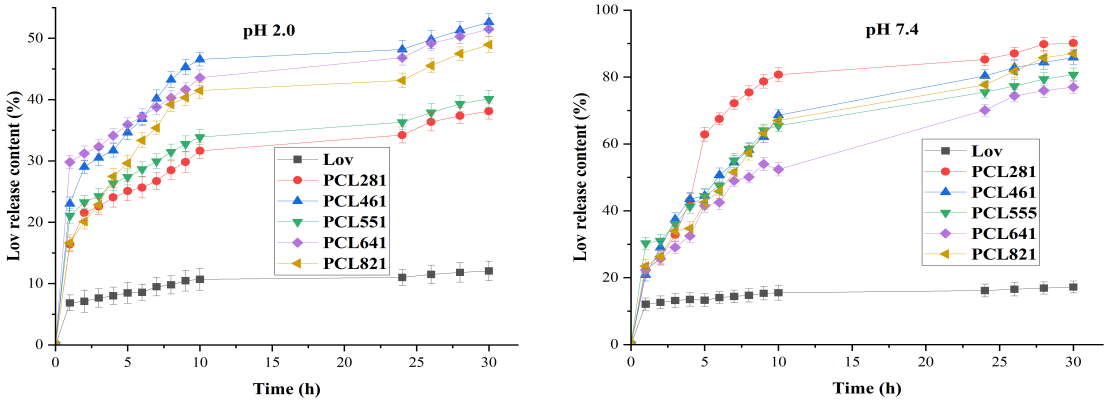

Figure 5. Lov content released in pH 2.0 (left) and pH 7.4 (right) buffer solutions.

The drug release process in pH 7.4 buffer also follows a biphasic pattern: in the initial stage, Lov molecules loosely bound to the polymer surface and are rapidly released. Subsequently, the release rate stabilizes as the drug diffuses through the polymer matrix. The swelling of the PLA/Carr polymer network in pH 7.4 solution facilitates the gradual fragmentation of PCL composites into small units, allowing for a sustained and controlled releases Lov into the solution. Specifically, after 30 hours of testing, the percentage of Lov released from PCL281, PCL461, PCL551, PCL641, and PCL821 composites reached 90.16 %, 85.84 %, 80.67 %, 76.99 %, and 87.01 %, respectively. This system exhibited a significantly better Lov release compared to PLA-based Lov carriers (54.25 %) [44], due to the hydrophobic nature of PLA, which limits its ability to carry and disperse Lov in the test buffer solution. The result also shows an improvement over the Carr-based Lov system (86.57 %) [54], indicating weak interactions between Carr and Lov. The PCL281 composite sample exhibited the highest Lov release in pH 7.4 buffer, which is attributed to its smallest and most uniformly dispersed particle size. This observation aligns with the DSC results: Lov in PCL281 had the lowest melting point (145.26 °C), consistent with a previous study [47]. Collectively, these findings indicate that PCL281 offers excellent Lov release performance, surpassing several other delivery systems. For example, a polycaprolactone (PCL) matrix coated with β-tricalcium phosphate (β-TCP) released ~80 % of its loaded Lov [55], and alginate–chitosan nanoparticles carrying Lov achieved ~70 % release [46], among others.

Considering the SEM, DSC, and drug release results, PCL281 demonstrated the highest Lov release at all time points among the composite samples, suggesting superior drug dispersion and polymer matrix compatibility. This enhanced compatibility may stem from molecular interactions (particularly hydrogen bonding) between components in the composite; for instance, hydrogen bonds may form between the C=O groups of PLA and the –OH groups of Carr, between the –OH group of Lov and the C=O or S=O groups of Carr, and between the –OH of Lov and the C=O of PLA. These interactions would improve the miscibility between Lov and the polymer matrix, promoting a more homogeneous drug distribution and thereby contributing to the improved release profile. These findings highlight that Lov release from the PCL composites is influenced by both the solution pH and the Carr/PLA ratio. The variations in drug release profiles across different formulations can be attributed to the distinct interaction among their components in the PCL composites. Notably, the PLA/Carr ratio of 2/8 demonstrated the most favorable release characteristics, as it provided effective drug protection in the acidic gastric environment (pH 2.0) while enabling optimal release and absorption in the intestinal environment (pH 7.4). Therefore, Lov tends to be poorly released at pH 2.0 and well released at pH 7.4.

4. CONCLUSIONS

In this study, lovastatin-loaded poly(lactic acid)/carrageenan composite systems were successfully synthesized using various component ratios. Structural (FTIR), morphological (SEM), thermal (DSC), and drug release (UV-Vis) characterizations confirmed that lovastatin was uniformly dispersed as nanoparticles (22–232 nm) within the polymer matrix, primarily due to hydrogen bonding and dipole-dipole interactions among the components. Among the formulations, the PCL281 sample (PLA/Carr = 2/8) exhibited the most favorable performance with several key features: The smallest and most uniform particle size (22–47 nm), as observed via SEM; The lowest melting point (145.26 °C), indicating a highly amorphous state, as shown by DSC; The lowest release rate at pH 2.0, suggesting effective protection of Lov in gastric conditions; The highest cumulative drug release at pH 7.4, reaching 90.16 % after 30 hours, which outperformed other tested formulations and several previously reported delivery systems. These findings demonstrate that the PCL281 composite is a promising pH-responsive carrier for the controlled oral delivery of lovastatin. Future studies should focus on evaluating the *in vitro* and *in vivo* biocompatibility, cytotoxicity, and pharmacokinetics of this optimized delivery system.

Credit authorship contribution statement. Vu Quoc Manh, Tran Thi Kieu Giang: Methodology. Vu Thi Thuong, Doan Thi Yen, Bui Thanh Nga, Huynh Xuan Mai, Pham Nguyen Thao Nguyen: Investigation. Nguyen Thi Hong Nhung, Nguyen Ngoc Linh: Formal analysis. Nguyen Thi Bich Viet, Vu Thi Huong, Nguyen Dang Dat: Writing – review & editing. Vu Quoc Trung: Writing – review & editing, Funding acquisition.

Declaration of competing interest. The authors declare that they have no known competing financial interests or personal relationships that could have appeared to influence the work reported in this paper.

REFERENCES

1. Chen Y., Geever L. M., Killion J. A., Lyons J. G., Higginbotham C. L., Devine D. M. – Review of multifarious applications of poly (lactic acid). Polym. Plast. Technol. Eng., **55** (2016) 1057–1075. https://doi.org/10.1080/03602559.2015.1132465.
2. Pawar R. P., Tekale S. U., Shisodia S., Totre J. T., Domb A. J. – Biomedical applications of poly(lactic acid). Recent Pat. Regen. Med., **4** (2014) 40–51. https://doi.org/10.2174/2210296504666140402235024.
3. Vlachopoulos A., Karlioti G., Balla E., Daniilidis V., Kalamas T., Stefanidou M., Bikiaris N. D., Christodoulou E., Koumentakou I., Karavas E., et al. – Poly(lactic acid)-based microparticles for drug delivery applications: an overview of recent advances. Pharmaceutics, **14** (2022) 359. https://doi.org/10.3390/pharmaceutics14020359.
4. DeStefano V., Khan S., Tabada A. – Applications of PLA in modern medicine. Eng. Regen., **1** (2020) 76–87. https://doi.org/10.1016/j.engreg.2020.08.002.
5. Mitragotri S., Burke P. A., Langer R. – Overcoming the challenges in administering biopharmaceuticals: formulation and delivery strategies. Nat. Rev. Drug Discov., **13** (2014) 655–672. https://doi.org/10.1038/nrd4363.
6. Nottelet B., Darcos V., Coudane J. – Aliphatic polyesters for medical imaging and theranostic applications. Eur. J. Pharm. Biopharm., **97** (2015) 350–370. https://doi.org/10.1016/j.ejpb.2015.06.023.
7. Tran T. T. T., Mariatti M., Badrul H. Y., Masakazu K., Nguyen X. T. T., Zuratul A. A. H. – Drug release profile study of gentamicin encapsulated poly(lactic acid) microspheres for drug delivery. Mater. Today Proc., **17** (2019) 836–845. https://doi.org/10.1016/j.matpr.2019.06.370.

8. Guan Q., Chen W., Hu X. – Development of lovastatin-loaded poly(lactic acid) microspheres for sustained oral delivery: *in vitro* and *ex vivo* evaluation. Drug Des. Devel. Ther., **9** (2015) 791–798. https://doi.org/10.2147/dddt.s76676.
9. Loca D., Sevostjanovs E., Makrecka M., Malkova O. Z., Cimdina L. B., Tupureina V., Sokolova M. – Microencapsulation of mildronate in biodegradable and non-biodegradable polymers. J. Microencapsul., **31** (2014) 246–253. https://doi.org/10.3109/02652048.2013.834992.
10. Ghosh B., Biswas S. – Polymeric micelles in cancer therapy: state of the art. J. Control. Release, **332** (2021) 127–147. https://doi.org/10.1016/j.jconrel.2021.02.016.
11. Xu J., Bai Y., Li X., Wei Z., Sun L., Yu H., Xu H. – Porous core/dense shell PLA microspheres embedded with high drug loading of bupivacaine crystals for injectable prolonged release. AAPS PharmSciTech, **22** (2021) 27. https://doi.org/10.1208/s12249-020-01878-8.
12. Zia K. M., Tabasum S., Nasif M., Sultan N., Aslam N., Noreen A., Zuber M. – A review on synthesis, properties and applications of natural polymer based carrageenan blends and composites. Int. J. Biol. Macromol., **96** (2017) 282–301. https://doi.org/10.1016/j.ijbiomac.2016.11.095.
13. McCandless E. L., Craigie J. S., Walter J. A. – Carrageenans in the gametophytic and sporophytic stages of *Chondrus crispus*. Planta, **112** (1973) 201–212. https://doi.org/10.1007/BF00385324.
14. Pacheco-Quito E.-M., Ruiz-Caro R., Veiga M.-D. – Carrageenan: drug delivery systems and other biomedical applications. Mar. Drugs, **18** (2020) 583. https://doi.org/10.3390/md18110583.
15. Yegappan R., Selvaprithiviraj V., Amirthalingam S., Jayakumar R. – Carrageenan-based hydrogels for drug delivery, tissue engineering and wound healing. Carbohydr. Polym., **198** (2018) 385–400. https://doi.org/10.1016/j.carbpol.2018.06.086.
16. Li L., Ni R., Shao Y., Mao S. – Carrageenan and its applications in drug delivery. Carbohydr. Polym., **103** (2014) 1–11. https://doi.org/10.1016/j.carbpol.2013.12.008.
17. Nguyen T. C., Tran T. M., Vu Q. M., Nguyen T. T. T., Do T. M. T., Vu Q. T., Ha V. H., Thai H. – Effect of fish scale collagen on some characteristics and drug release of carrageenan/collagen/allopurinol film. Vietnam J. Sci. Technol., **57** (2019) 1–8. https://doi.org/10.15625/2525-2518/57/3B/14044.
18. Nguyen T. C., Vu Q. M., Phan T. T., Vu Q. T., Vo A. Q., Bach L. G., Thai H. – Novel pH-sensitive hydrogel beads based on carrageenan and fish scale collagen for allopurinol drug delivery. J. Polym. Environ., **28** (2020) 1795–1810. https://doi.org/10.1007/s10924-020-01727-6.
19. Nguyen T. C., Vu Q. M., Thai H., Kavitha R., Sathish C. I., Vu Q. T., Tran T. K. N., Ajayan V. – Optimizing the component ratio to develop the biocomposites with carrageenan/collagen/allopurinol for the controlled drug release. J. Drug Deliv. Sci. Technol., **68** (2022) 102697. https://doi.org/10.1016/j.jddst.2021.102697.
20. Vu Q. M., Nguyen T. C., Dam D. M. N., Vu Q. T., Le T. L., Hoang T. D., Tram T. K. N., Nguyen T. A., Nguyen P. H., Thai H. – A novel method for preparation of carrageenan/fish scale collagen/allopurinol biocomposite film. Int. J. Polym. Sci., **2021** (2021) 1–10. https://doi.org/10.1155/2021/9960233.
21. Madruga L. Y. C., Sabino R. M., Santos E. C. G., Popat K. C., Balaban R. de C., Kipper M. J. – Carboxymethyl-κ-carrageenan: a study of biocompatibility, antioxidant and antibacterial activities. Int. J. Biol. Macromol., **152** (2020) 483–491. https://doi.org/10.1016/j.ijbiomac.2020.02.274.
22. Boulho R., Marty C., Freile-Pelegrín Y., Robledo D., Bourgougnon N., Bedoux G. – Antiherpetic (HSV-1) activity of carrageenans from the red seaweed *Solieria chordalis* (*Rhodophyta*, *Gigartinales*) extracted by microwave-assisted extraction (MAE). J. Appl. Phycol., **29** (2017) 2219–2228. https://doi.org/10.1007/s10811-017-1192-5.
23. Besednova N., Zaporozhets T., Kuznetsova T., Makarenkova I., Fedyanina L., Kryzhanovsky S., Malyarenko O., Ermakova S. – Metabolites of seaweeds as potential agents for the prevention and therapy of influenza infection. Mar. Drugs, **17** (2019) 373. https://doi.org/10.3390/md17060373.
24. Shi Q., Wang A., Lu Z., Qin C., Hu J., Yin J. – Overview on the antiviral activities and mechanisms of marine polysaccharides from seaweeds. Carbohydr. Res., **453–454** (2017) 1–9. https://doi.org/10.1016/j.carres.2017.10.020.
25. Perino A., Consiglio P., Maranto M., De Franciscis P., Marci R., Restivo V., Manzone M., Capra G., Cucinella G., Calagna G. – Impact of a new carrageenan-based vaginal microbicide in a female

population with genital HPV-infection: first experimental results. Eur. Rev. Med. Pharmacol. Sci., **23** (2019) 6744–6752. https://doi.org/10.26355/eurrev_201908_18567.
26. Ugaonkar S. R., Wesenberg A., Wilk J., Seidor S., Mizenina O., Kizima L., Rodriguez A., Trương T. D., Levendosky K., Kenney J., et al. – A novel intravaginal ring to prevent HIV-1, HSV-2, HPV, and unintended pregnancy. J. Control. Release, **213** (2015) 57–68. https://doi.org/10.1016/j.jconrel.2015.06.018.
27. Chen F., Deng Z., Zhang Z., Zhang R., Xu Q., Fan G., Luo T., McClements D. J. – Controlling lipid digestion profiles using mixtures of different types of microgel: alginate beads and carrageenan beads. J. Food Eng., **238** (2018) 156–163. https://doi.org/10.1016/j.jfoodeng.2018.06.009.
28. Sokolova E. V., Kravchenko A. O., Sergeeva N. V., Davydova V. N., Bogdanovich L. N., Yermak I. M. – Effect of carrageenans on some lipid metabolism components *in vitro*. Carbohydr. Polym., **230** (2020) 115629. https://doi.org/10.1016/j.carbpol.2019.115629.
29. Valado A., Pereira M., Caseiro A., Figueiredo J. P., Loureiro H., Almeida C., Cotas J., Pereira L. – Effect of carrageenans on vegetable jelly in humans with hypercholesterolemia. Mar. Drugs, **18** (2019) 19. https://doi.org/10.3390/md18010019.
30. Liang W., Mao X., Peng X., Tang S. – Effects of sulfate group in red seaweed polysaccharides on anticoagulant activity and cytotoxicity. Carbohydr. Polym., **101** (2014) 776–785. https://doi.org/10.1016/j.carbpol.2013.10.010.
31. Dos Santos-Fidencio G. C., Gonçalves A. G., Noseda M. D., Duarte M. E. R., Ducatti D. R. B. – Effects of carboxyl group on the anticoagulant activity of oxidized carrageenans. Carbohydr. Polym., **214** (2019) 286–293. https://doi.org/10.1016/j.carbpol.2019.03.057.
32. Calvo G. H., Cosenza V., Sáenz D. A., Navarro D. A., Stortz C. A., Céspedes M. A., Mamone L. A., Casas A. G., Di V. G. M. – Disaccharides obtained from carrageenans as potential antitumor agents. Sci. Rep., **9** (2019) 6654. https://doi.org/10.1038/s41598-019-43238-y.
33. Cicinskas E., Begun M. A., Tiasto V. A., Belousov A. S., Vikhareva V. V., Mikhailova V. A., Kalitnik A. A. – *In vitro* antitumor and immunotropic activity of carrageenans from red algae *Chondrus armatus* and their low-molecular weight degradation products. J. Biomed. Mater. Res., **108** (2020) 254–266. https://doi.org/10.1002/jbm.a.36812.
34. Liu Z., Gao T., Yang Y., Meng F., Zhan F., Jiang Q., Sun X. – Anti-cancer activity of porphyran and carrageenan from red seaweeds. Molecules, **24** (2019) 4286. https://doi.org/10.3390/molecules24234286.
35. Samuel M. C., Nobuyuki I. – A critical review of the toxicological effects of carrageenan and processed eucheuma seaweed on the gastrointestinal tract. Crit. Rev. Toxicol., **32** (2002) 413–444. https://doi.org/10.1080/20024091064282.
36. Myra L. W., David N., William R. B., Jay F. H., Samuel M. C. – A 90-day dietary study on κ-carrageenan with emphasis on the gastrointestinal tract. Food Chem. Toxicol., **45** (2007) 98–106. https://doi.org/10.1016/j.fct.2006.07.033.
37. Gunde-Cimerman N., Cimerman A. – *Pleurotus* fruiting bodies contain the inhibitor of 3-hydroxy-3-methylglutaryl-coenzyme A reductase-lovastatin. Exp. Mycol., **19** (1995) 1–6. https://doi.org/10.1006/emyc.1995.1001.
38. Liu J., Zhang J., Shi Y., Grimsgaard S., Alraek T., Fønnebø V. – Chinese red yeast rice (*Monascus purpureus*) for primary hyperlipidemia: a meta-analysis of randomized controlled trials. Chin. Med., **1** (2006) 4. https://doi.org/10.1186/1749-8546-1-4.
39. Li Z., Seeram N. P., Lee R., Thames G., Minutti C., Wang H.-J., Heber D. – Plasma clearance of lovastatin versus Chinese red yeast rice in healthy volunteers. J. Altern. Complement. Med., **11** (2005) 1031–1038. https://doi.org/10.1089/acm.2005.11.1031.
40. Zolkiflee N. F., Meor Mohd Affandi M. M. R., Majeed A. B. A. – Lovastatin: history, physicochemistry, pharmacokinetics and enhanced solubility. Int. J. Res. Pharm. Sci., **8** (2017) 90–102.
41. Vo A. Q., Nguyen T. C., Nguyen Q. T., Vu Q. T., Truong C. D., Nguyen T. L., Ly T. N. L., Bach L. G., Thai H. – Novel nanoparticle biomaterial of alginate/chitosan loading simultaneously lovastatin and ginsenoside RB1: characteristics, morphology, and drug release study. Int. J. Polym. Sci., **2021** (2021) 1–14. https://doi.org/10.1155/2021/5214510.

42. Vu T. T. T., Nguyen T. H. N., Vu Q. M., Nguyen N. L., Nguyen T. B. V., Vu Q. T. – Synthesis and characterization of chitosan/carrageenan/polyaniline-based biocomposite as lovastatin carrier and its drug release ability. HNUE J. Sci., **68** (2023) 64–74. https://doi.org/10.18173/2354-1059.2023-0061.
43. Ha M. H., Vu Q. M., Vu T. T. T., Dao T. P. T., Pham T. D., Nguyen T. B. V., Duong K. L., Nguyen N. L., Doan T. Y. O., Nguyen T. C., et al. – Evaluation of the effect of the chitosan/carrageenan ratio on lovastatin release from chitosan/carrageenan-based biomaterials. Vietnam J. Chem., **60** (2022) 72–78. https://doi.org/10.1002/vjch.202200078.
44. Nguyen T. B. V., Vu Q. M., Tran T. K. G., Doan T. Y., Vu T. H., Ha M. H., Nguyen D. D., Vu Q. T., Nguyen N. L. – Release of lovastatin drug from poly(lactic acid) biomaterial. Vietnam J. Chem. Appl., **3B** (2024) 23–30.
45. Chen Z., Xiao L., Hu C., Shen Z., Zhou E., Zhang S., Wang Y. – Aligned lovastatin-loaded electrospun nanofibers regulate collagen organization and reduce scar formation. Acta Biomater., **164** (2023) 240–252. https://doi.org/10.1016/j.actbio.2023.04.015.
46. Hoang T., Nguyen T. C., Thach T. L., Tran T. M., Mai D. H., Nguyen T. T. T., Le D. G., Can V. M., Tran D. L., Bach L. G., et al. – Characterization of chitosan/alginate/lovastatin nanoparticles and investigation of their toxic effects *in vitro* and *in vivo*. Sci. Rep., **10** (2020) 909. https://doi.org/10.1038/s41598-020-57666-8.
47. Thai H., Tran D. L., Thach T. L., Le D. G., Tran D. M. T., Vu Q. T., Nguyen T. A., Nguyen D. T., Nguyen T. C. – Effect of both lovastatin and ginsenoside Rb1 on some properties and *in-vitro* drug release of alginate/chitosan/lovastatin/ginsenoside Rb1 composite films. J. Polym. Environ., **27** (2009) 2728–2738. https://doi.org/10.1007/s10924-019-01550-8.
48. Abdel A. F. H., Mohamed N. A., Ali H. R. H. – FTIR spectroscopic study of two isostructural statins: simvastatin and lovastatin as authentic and in pharmaceuticals. Spectrochim. Acta A Mol. Biomol. Spectrosc., **261** (2021) 120045. https://doi.org/10.1016/j.saa.2021.120045.
49. Zhou B., Hu S., Zhang P. – Isothermal crystalline polymorphs of poly(l-lactic acid) by FTIR coupled with two-dimensional correlation spectroscopy and perturbation-correlation moving-window two-dimensional analysis. Spectrochim. Acta A Mol. Biomol. Spectrosc., **229** (2020) 117953. https://doi.org/10.1016/j.saa.2019.117953.
50. Hung H. M., Manh V. Q., Thao V. T. T., Thuy D. T. P., Dung P. T., Viet N. T. B., Linh D. K., Linh N. N., Oanh D. T. Y., Chinh N. T., et al. – Evaluation of the effect of the chitosan/carrageenan ratio on lovastatin release from chitosan/carrageenan based biomaterials. Vietnam Journal of Chemistry, **60** (2022) 72–78. https://doi.org/10.1002/vjch.202200078.
51. Yoshida M. I., Oliveira M. A., Gomes E. C. L., Mussel W. N., Castro W. V., Soares C. D. V. – Thermal characterization of lovastatin in pharmaceutical formulations. J. Therm. Anal. Calorim., **106** (2011) 657–664. https://doi.org/10.1007/s10973-011-1510-0.
52. Jose M. F., Daniel G. G., Emilio R., Maria D. S., Rafael B. – Compatibilization and characterization of polylactide and biopolyethylene binary blends by non-reactive and reactive compatibilization approaches. Polymers, **12** (2020) 1344. https://doi.org/10.3390/polym12061344.
53. Zakuwan S. Z., Ahmad I. – Effects of hybridized organically modified montmorillonite and cellulose nanocrystals on rheological properties and thermal stability of κ-carrageenan bio-nanocomposite. Nanomaterials, **9** (2019) 1547. https://doi.org/10.3390/nano9111547.
54. Vu Q. M., Vu T. T., Doan T. Y., Le T. D., Nguyen N. L., Nguyen T. B. V., Nguyen D. D., Vu Q. T. – Preparation and characterization of carrageenan/lovastatin biomaterials. HNUE J. Sci., **70** (2025) 3–10.
55. Solaiman T., Kelly N., Susmita B. – Lovastatin release from polycaprolactone coated β-tricalcium phosphate: effects of pH, concentration and drug-polymer interactions. Mater. Sci. Eng. C, **33** (2013) 3121–3128. https://doi.org/10.1016/j.msec.2013.02.049.